Synthesis and Properties of *Ortho*-Linked Aromatic Polyimides Based on 1,2-Bis(4-aminophenoxy)-4-*tert*-butylbenzene

SHENG-HUEI HSIAO, CHIN-PING YANG, SHIN-HUNG CHEN

Department of Chemical Engineering, Tatung University, 40 Chuangshan North Road, Sec. 3, Taipei, Taiwan, Republic of China

Received 8 November 1999; accepted 1 February 2000

ABSTRACT: A bis(ether amine) containing the *ortho*-substituted phenylene unit and pendant *tert*-butyl group, 1,2-bis(4-aminophenoxy)-4-*tert*-butylbenzene, was synthesized and used as a monomer to prepare polyimides with six commercial dianhydrides via a conventional two-stage procedure. The intermediate poly(amic acid)s had inherent viscosities of 0.78–1.44 dL/g, and most of them could be thermally converted into transparent, flexible, and tough polyimide films. The inherent viscosities of the resulting polyimides were in the range of 0.46–0.87 dL/g. All polyimides were noncrystalline, and most of them showed excellent solubility in polar organic solvents. The glass-transition temperatures of these polyimides were in the range of 222–259 °C in differential scanning calorimetry and 212–282 °C in thermomechanicl analysis. These polyimides showed no appreciable decomposition up to 500 °C in thermogravimetric analysis in air or nitrogen. A comparative study of the properties with the corresponding polyimides without pendant *tert*-butyl groups derived from 1,2-bis(4-aminophenoxy)-benzene is also presented. © 2000 John Wiley & Sons, Inc. J Polym Sci A: Polym Chem 38: 1551–1559, 2000

Keywords: 1,2-bis(4-aminophenoxy)benzene; 1,2-bis(4-aminophenoxy)-4-*tert*-butylbenzene; *ortho*-linked; polyimide

INTRODUCTION

Aromatic polyimides have been noted for their outstanding thermal stability and electrical properties.[1,2] Some of these materials have been widely used in industry as structural materials and integrated circuit insulators. However, they are usually difficult to directly process in their imidized forms because of their high glass-transition (T_g) and melting temperatures and their limited solubility, which limits their usefulness for many applications. Several modifications of the chemical structure have been made to improve the solubility and processability of polyimides with minimal detrimental effect to their high thermal stability. The incorporation of flexible segments, bulky pendant groups, and sterically hindered structures has been successful in decreasing crystallinity and intermolecular interactions to increase solubility and tractability.[3–11]

Another approach to increasing the solubility of polyimides is the incorporation of less symmetric, such as *meta*- or *ortho*-catenated, aromatic units in the main chains.[12–16] We reported that the nucleophilic chloro-displacement reaction between *p*-chloronitrobenzene with *ortho*-substituted aromatic diols such as catechol and 2,3-dihydroxynaphthalene could successfully proceed to form the *ortho*-linked dinitro compounds, which could be readily reduced to the *ortho*-linked

Correspondence to: S.-H. Hsiao

Journal of Polymer Science: Part A: Polymer Chemistry, Vol. 38, 1551–1559 (2000)

diamines used in polyamide and polyimide synthesis.[16–18] The lateral arrangement of *ortho*-linked aromatic moieties, especially the 2,3-naphthalenediyl unit, could interrupt interchain packing, reduce T_g, and increase solubility. Recently, we studied polyimides derived from 1,2-bis(4-aminophenoxy)benzene, a catechol-based bis(ether amine), with commercial dianhydrides in an effort to enhance the solubility. However, unless 2,2-bis(3,4-dicarboxyphenyl)hexafluoropropane dianhydride (6FDA) was incorporated, these polyimides were not organosoluble. Several previous articles[19–25] have demonstrated that introducing a *tert*-butyl substituted monomer into the polymer backbone improves processability significantly without an unacceptable loss of thermal properties in many aromatic polymer systems such as polyarylates, polyamides, polyimides, and poly(amide-imide)s. This article describes the synthesis and basic characterization of polyimides based on 1,2-bis(4-aminophenoxy)-4-*tert*-butylbenzene. Analogous polyimides based on 1,2-bis(4-aminophenoxy)benzene were also synthesized for comparison. *tert*-Butyl-substituted bis(ether amine) was previously reported by Eastmond and Paprotny[26] in 1998; however, little is known about the synthesis and properties of polymers from this diamine monomer to date. It was hoped that the incorporation of both the *ortho*-catenated phenylene unit and the bulky *tert*-butyl group would decrease polymer interchain interactions and generally disturb the coplanarity of aromatic units to reduce packing efficiency and crystallinity. This should promote solubility while maintaining high T_g's through controlled segmental mobility.

EXPERIMENTAL

Materials

Catechol (Acros), 4-*tert*-butylcatechol (Acros), *p*-chloronitrobenzene, 10% palladium on activated carbon (Pd/C; Fluka), and hydrazine monohydrate (Acros) were used as received. Pyromellitic dianhydride (PMDA; **4a**; Aldrich), 3,3′,4,4′-benzophenonetetracarboxylic dianhydride (**4c**; Aldrich), 4,4′-oxydiphthalic anhydride (OPDA; **4d**; Oxychem), and diphenylsulfone-3,3′,4,4′-tetracarboxylic dianhydride (DSDA; **4e**; New Japan Chemical Co.) were recrystallized from acetic anhydride before use. 3,3′,4,4′-Biphenyltetracarboxylic dianhydride (BPDA; **4b**; Oxychem) and 6FDA (**4f**; Hoechst) were purified by sublimation. *N*,*N*-Dimethylacetamide (DMAc) was purified by distillation under reduced pressure over calcium hydride and stored over 4-Å molecular sieves.

Monomer Synthesis

1,2-Bis(4-aminophenoxy)benzene (**3a**) and 1,2-bis(4-aminophenoxy)-4-*tert*-butylbenzene (**3b**) were prepared in two steps by the aromatic nucleophilic displacement reaction of the corresponding catechols with *p*-chloronitrobenzene to give dinitro compounds **2a** and **2b**, followed by reduction with hydrazine hydrate/Pd–C. A detailed procedure for the preparation of diamine **3b** follows.

4-tert-Butyl-1,2-bis(4-nitrophenoxy)benzene (2b)

4-*tert*-Butylcatechol (33.2 g, 0.2 mol) and *p*-chloronitrobenzene (63 g, 0.4 mol) were dissolved in 200 mL of *N*,*N*-dimethylformamide (DMF) in a 500-mL round-bottom flask with stirring. Then, potassium carbonate (55.2 g, 0.4 mol) was added, and the suspension mixture was refluxed at 140 °C for 12 h. The mixture was allowed to cool and subsequently poured into 500 mL of methanol/water (1/1 by volume). The crude product was recrystallized from DMF/water to give pure 4-*tert*-butyl-1,2-bis(4-nitrophenoxy)benzene (**2b**).

Yield: 54% (47.3 g). mp: 147–149 °C by differential scanning calorimetry (DSC; lit.[26] 147.2–147.9 °C). IR (KBr): 2964 (aliphatic C—H str.), 1514 (asym. —NO_2 str.), 1342 (sym. —NO_2 str.), 1224 cm^{-1} (C—O—C str.). ^1H NMR (DMSO-d_6, δ, ppm): 8.16 [two overlapped AB doublets (2d), 4H, $H_e + H_{e'}$], 7.45 (d, 1H, H_b), 7.38 (s, 1H, H_a), 7.30 (d, 1H, H_c), 6.96 (2d, 4H, $H_d + H_{d'}$), 1.35 (s, 9H, *t*-butyl). ^{13}C NMR (DMSO-d_6, δ, ppm): 161.99, 161.90 (C^9, $C^{9'}$), 150.45 (C^4), 144.45 (C^2), 142.72 (C^1), 142.19, 141.12 (C^{12}, $C^{12'}$), 125.65, 125.47 (C^{11}, $C^{11'}$), 123.96 (C^6), 122.48 (C^3), 120.17 (C^5), 116.21, 116.04 (C^{10}, $C^{10'}$), 34.52 (C^7), 30.99 (C^8).

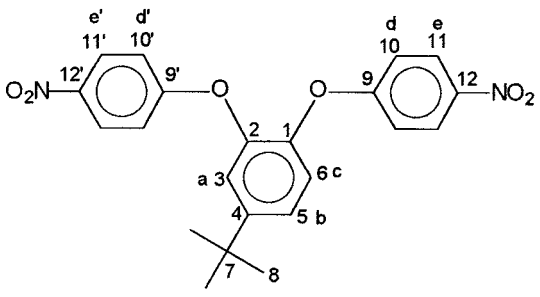

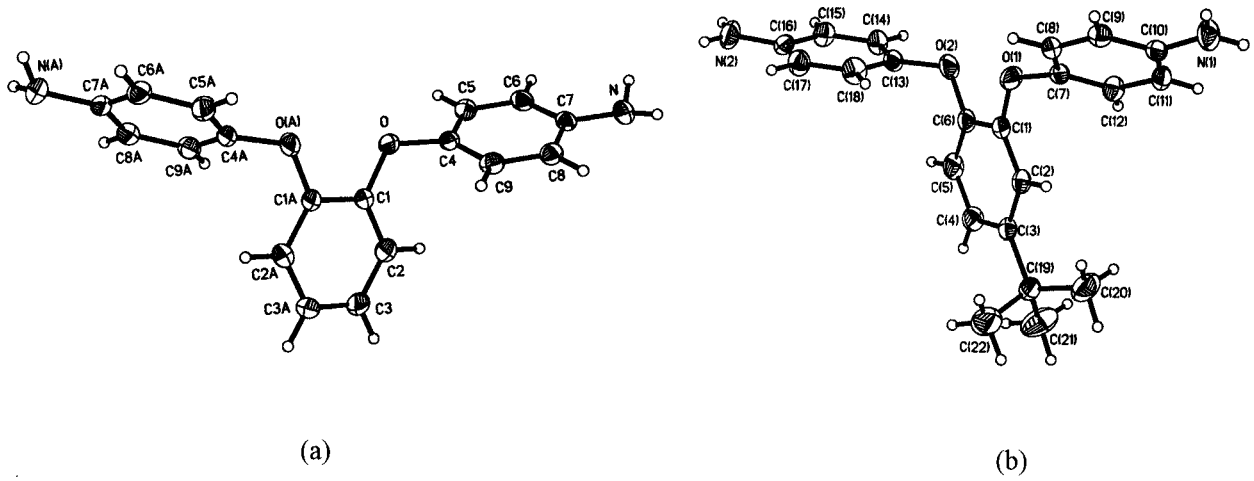

Figure 1. X-ray structures of diamines (a) **3a** and (b) **3b**.

ELEM. ANAL. Calcd. for $C_{22}H_{20}N_2O_6$ (408.41): C, 64.70%; H, 4.97%; N, 6.86%. Found: C, 64.47%; H, 4.92%; N, 6.81%.

1,2-Bis(4-aminophenoxy)-4-tert-Butylbenzene (3b)

A mixture of the obtained dinitro compound **2b** (22.3 g, 0.0546 mol), 10% Pd/C (0.1 g), and ethanol (200 mL) was heated to reflux. Then, 60 mL of hydrazine hydrate was added dropwise into the suspension solution over a period of 1 h. After complete addition, the mixture was heated at reflux temperature for an additional 6 h. The reaction solution was then filtered to remove Pd/C. The crude product was recrystallized from ethanol to give colorless needles.

Yield: 86% (16.3 g). mp: 129–131 °C by DSC (lit.[26] 131–132 °C). IR (KBr): 3422, 3322, 3216 (N—H str.), 2966 (aliphatic C—H str.), 1193 cm^{-1} (C—O—C str.). ^1H NMR ($CDCl_3$, δ, ppm): 6.99 (s, 1H, H_a), 6.97 (d, 1H, H_b), 6.82 (d, 1H, H_c), 6.78 (2d, 4H, $H_d + H_{d'}$), 6.58 (2d, 4H, $H_e + H_{e'}$), 3.41 (s, 4H, —NH_2), 1.23 (s, 9H, *t*-butyl). ^{13}C NMR ($CDCl_3$, δ, ppm): 149.50 (C^4), 149.08 (C^2), 146.90 (C^1), 146.36, 146.06 (C^9, $C^{9'}$), 141.68, 141.36 (C^{12}, $C^{12'}$), 119.96 (C^6), 119.38, 118.68 (C^{10}, $C^{10'}$), 118.43 (C^3), 117.18 (C^5), 115.80, 115.74 (C^{11}, $C^{11'}$), 34.26 (C^7), 31.26 (C^8).

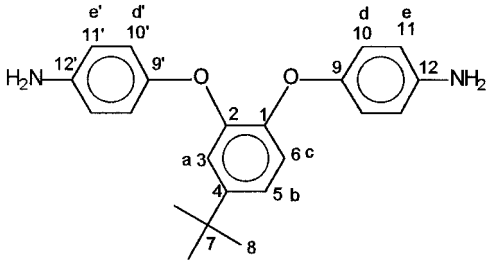

ELEM. ANAL. Calcd. for $C_{22}H_{24}N_2O_2$ (348.44): C, 75.83%; H, 6.94%; N, 8.04%. Found: C, 75.81%; H, 6.97%; N, 7.87%.

X-Ray Structure Analysis

The single crystals of diamines were grown during the slow crystallization of their ethanol solutions. Crystal sizes of 0.35 × 0.40 × 0.45 mm for diamine **3a** and 0.65 × 0.30 × 0.12 mm for **3b** were used for X-ray structure determination. Intensity data were collected on an Enraf–Norius FR 590 CAD-4 diffractometer at 293 K with graphite monochromatized Mo K_α radiation (λ = 0.71073 Å). Diamine **3a** crystallized in a monoclinic system with space group C2 [M_w = 292.33; a = 18.111(3), b = 7.193(3), c = 5.7222(11) Å; β = 103.054(15)° where D_c = 1.337 g/cm^3 for Z = 4 and V = 726.1(3) $Å^3$]. Diamine **3b** crystallized in a monoclinic system with space group $P2_1/c$ [M_w = 348.44; a = 14.509(3), b = 9.535(2), c = 13.815(3) Å; α = 90, β = 98.08(3), γ = 90° where D_c = 1.223 g/cm^3 for Z = 4 and V = 1892.4(7) $Å^3$]. Least-squares refinement based on 3324 independent reflections converged to final R_1 = 0.0478 and R_w = 0.1179.

The structure was solved on a VAX-3300 computer with NRCC SDP (Structure Determination Package) software. The molecular structure for diamine **3a** is shown in Figure 1(a). The bond lengths (Å) are the following: O—C1, 1.378(3); O—C4, 1.3974(22); N—C7, 1.394(3); C1—C1a, 1.386(4); C1—C2, 1.380(4); C2—C3, 1.381(4); C3—C3a, 1.370(5); C4—C5, 1.382(3); C4—C9, 1.365(3); C5—C6, 1.378(3); C6—C7, 1.381(3); C7—C8, 1.395(3); and C8—C9, 1.382(3). The bond

angles (°) are the following: C1—O—C4, 119.15(16); O—C1—C1a, 116.26(23); O—C1—C2, 124.10(18); C1a—C1—C2, 119.59(24); C1—C2—C3, 120.38(20); C2—C3—C3a 120.0(3); O—C4—C5, 117.17(20); O—C4—C9, 122.31(20); C5—C4—C8, 120.31(18); C4—C5—C6, 119.66(21); C5—C6—C7, 121.23(21); N—C7—C6, 120.74(21); N—C7—C8, 121.21(21); C6—C7—C8, 118.01(18); C7—C8—C9, 120.90(21); and C4—C9—C8, 119.87(20). The molecular structure for diamine **3b** is shown in Figure 1(b). The bond lengths (Å) are the following: O1—C1, 1.378(3); O2—C6, 1.385(3); N1—C10, 1.403(3); C1—C2, 1.374(3); C2—C3, 1.396(3); C3—C19, 1.523(4); C5—C6, 1.368(4); C7—C12, 1.376(3); C9—C10, 1.378(3); C11—C12, 1.385(3); C13—C18, 1.366(4); C15—C16, 1.374(4); C17—C18, 1.382(4); C19—C20, 1.522(4); O1—C7, 1.398(3); O2—C13, 1.405(3); N2—C16, 1.398(3); C1—C6, 1.389(3); C3—C4, 1.383(4); C4—C5, 1.380(4); C7—C8, 1.366(3); C8—C9, 1.374(3); C10—C11, 1.385(3); C13—C14, 1.356(3); C14—C15, 1.387(3); C16—C17, 1.381(4); C19—C21, 1.507(4); and C19—C22, 1.533(4). The bond angles (°) are the following: C1—O1—C7, 120.6(2); C2—C1—O1, 124.7(2); O1—C1—C6, 115.5(2); C4—C3—C2, 116.4(2); C2—C3—C19, 121.4(2); C6—C5—C4, 121.1(3); C5—C6—C1, 118.8(2); C8—C7—C12, 120.3(2); C12—C7—O1, 120.3(2); C12—C7—O1, 122.3(2); C8—C9—C10, 120.9(2); C9—C10—N1, 122.0(2); C12—C11—C10, 121.2(2); C14—C13—C18, 120.1(2); C18—C13—O2, 120.3(2); C16—C15—C14, 120.8(2); C15—C16—N2, 120.9(2); C16—C17—C18, 120.7(3); C21—C19—C20, 107.8(3); C20—C19—C3, 111.7(2); C20—C19—C22, 107.1(3); C6—O2—C13, 115.8(2); C2—C1—C6, 119.6(2); C1—C2—C3, 122.5(2); C4—C3—C19, 122.1(2); C5—C4—C3, 121.6(3); C5—C6—O2, 122.5(2); O2—C6—C1, 118.7(2); C8—C7—O1, 117.1(2); C7—C8—C9, 120.2(2); C9—C10—C11, 118.2(2); C11—C10—N1, 119.8(2); C7—C12—C11, 119.0(2); C14—C13—O2, 119.5(2); C13—C14—C15, 120.2(3); C15—C16—C17, 118.2(2); C17—C16—N2, 120.8(3); C13—C18—C17, 120.0(3); C21—C19—C3, 112.0(3); C21—C19—C22, 108.9(3); and C3—C19—C22, 109.2(2).

Polymer Synthesis

A typical example of polymerization was as follows. To a solution of 0.6150 g (1.765 mmol) of diamine **3b** in 9.5 mL of dried DMAc in a 50-mL flask, 0.3850 g (1.765 mmol) of PMDA was added in one portion. The mixture was stirred at room temperature for 3 h to afford a viscous poly(amic acid) solution. The inherent viscosity of the resulting poly(amic acid) **6a** was 1.44 dL/g, as measured in DMAc at a concentration of 0.5 g/dL at 30 °C. The polymer solution was spread on a 9-cm glass culture dish that was placed overnight in a 90 °C oven to remove most of the solvent. The semidried poly(amic acid) film was further dried and transformed into polyimide **8a** by the following heating program: 150 °C for 20 min, 180 °C for 20 min, 210 °C for 30 min, 230 °C for 30 min, 250 °C for 30 min, and 270 °C for 30 min. The polyimide film was released from the glass substrate by being soaked in hot water. The inherent viscosity of polyimide **8a** was 0.87 dL/g in concentrated sulfuric acid at a concentration of 0.5 g/dL at 30 °C.

Measurements

IR spectra were recorded on a Jasco FT/IR-7000 Fourier transform infrared (FTIR) spectrometer. NMR spectra were obtained on a JEOL EX-400 spectrometer. The inherent viscosity was measured with an Ubbelohde viscometer at 30 °C. DSC was performed on a Perkin–Elmer DSC 7 with a heating rate of 20 °C/min for normal scans and 5 °C/min for the melting point determination of the synthetic compounds. T_g's were read at the middle of the change in the heat capacity and were taken from the second heating scan after quenching from 400 °C. Thermomechanical analysis (TMA) was performed on a Perkin–Elmer TMA 7 with a loaded penetration probe (static force = 30 mN). The TMA experiments were conducted in duplicate from 30 to 300 °C at a scan rate of 10 °C/min. The apparent T_g was taken as the onset temperature of probe penetration from the second TMA traces. Thermogravimetric analysis (TGA) was conducted with a TA Instruments TGA 2050. Experiments were carried out on approximately 10 mg of the samples in flowing nitrogen or air (flow rate = 100 cm^3/min) at a heating rate of 20 °C/min. Wide-angle X-ray diffraction measurements were performed at room temperature (about 25 °C) on a Siemens Kristalloflex D5000 X-ray diffractometer with Ni-filtered Cu K_α radiation (λ = 1.5418 Å) operating at 40 kV and 20 mA. The scanning rate was 2°/min over a range of 2θ = 5–45°. An Instron Model 1130 universal testing machine with a 5-kg load cell was used to study the stress–strain behavior of the polyimide films (6 cm long, 0.5 cm wide, and approximately 0.08 mm thick) with a crosshead gauge length of 2 cm and a crosshead rate of 1

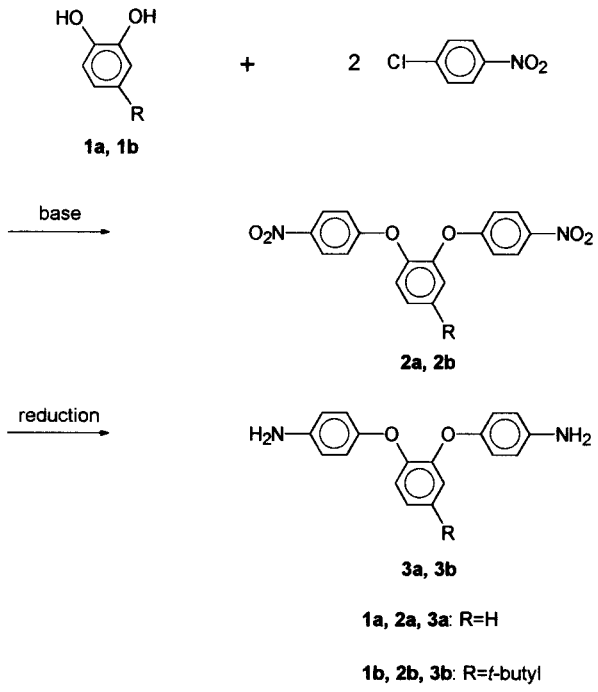

Scheme 1

mm/min. An average of at least five individual determinations was used.

RESULTS AND DISCUSSION

Monomer Synthesis

1,2-Bis(4-aminophenoxy)benzene (**3a**) and 1,2-bis(4-aminophenoxy)-4-*tert*-butylbenzene (**3b**) were prepared in two steps according to Scheme 1. Intermediate dinitro compounds **2a** and **2b** were synthesized by the nucleophilic aromatic substitution of *p*-chloronitrobenzene with catechol (**1a**) and 4-*tert*-butylcatechol (**1b**), respectively, in the presence of anhydrous potassium carbonate in DMF. The diamines **3a** and **3b** were readily obtained by the catalytic reduction of the dinitro compounds **2a** and **2b** with hydrazine hydrate and Pd/C catalyst in refluxing ethanol. Recently, Eastmond and Paprotny[26] also synthesized diamine **3b**, which was prepared by a fluoro-displacement reaction between *p*-fluoronitrobenzene and 4-*tert*-butylcatechol followed by a Pd/C-catalyzed hydrazine reduction of the resulting dinitro compound. For the syntheses of dinitrophenxy compounds reported here, we preferred to use chloro-displacement reactions from *p*-chloronitrobenzene rather than the more expensive *p*-fluoronitrobenzene because of the comparable yields and purity of the products. As shown in the Experimental section, FTIR, NMR, and elemental analysis confirmed the structures of the intermediate **2b** and diamine **3b**. The characterization data of dinitro compound **2a** and diamine **3a** are as reported.[18] The chemical structures of the diamine monomers were further detailed by a single-crystal X-ray diffraction analysis (Fig. 1). The crystal structures of the diamines show that the terminal phenylene rings are nearly orthogonal to the central phenylene ring. Eastmond and Paprotny[12] used a molecular modeling method and obtained similar conformations of diphenoxyphenyl units present in catechol-based bis(ether anhydride) and poly(ether-imide)s. Relative to **3a** (V = 726.1 Å^3, Z = 4), **3b** inevitably occupies a larger volume (V = 1892.4 Å^3, Z = 4) because of *tert*-butyl groups.

Polymer Synthesis

Aromatic polyimides **8a–f** were prepared by the classical two-step procedure from diamine **3b** with six commercially available dianhydrides, **4a–f**, via poly(amic acid)s **6a–f**, followed by thermal imidization (Scheme 2). For comparison, polyimides **7a–f** were prepared from diamine **3a** with dianhydrides **4a–f** with the same process. Polymer preparation involved adding a solid dianhydride to the diamine solution in dry DMAc to form the poly(amic acid), spreading the poly(amic acid) solution onto a glass substrate, slowly evaporating the solvent, and finally thermally dehydrating to form the polyimide. Thus, all the polyimides were obtained in the form of films. Completion of the imidization by the heating program shown in the Experimental section was confirmed by dynamic TGA of a sample of the poly(amic acid). The weight loss was complete around 250 °C, and the thermogravimetric curve of a sample showed no difference from the curve of a sample imidized as a film on a glass substrate. As shown in Table I, the inherent viscosities of the intermediate poly(amic acid)s were in the range of 0.78–1.86 dL/g, indicating the formation of high molecular weight. The casting films of polyimides **7a** and **8a** that were derived from PMDA cracked upon creasing, possibly because of the rigid nature of these polyimides. The other polyimides afforded good-quality, creasable films. Most of the polyimides with the pendant *tert*-butyl group exhibited excellent solubility in polar solvents such as DMAc. Therefore, the characterization of in-

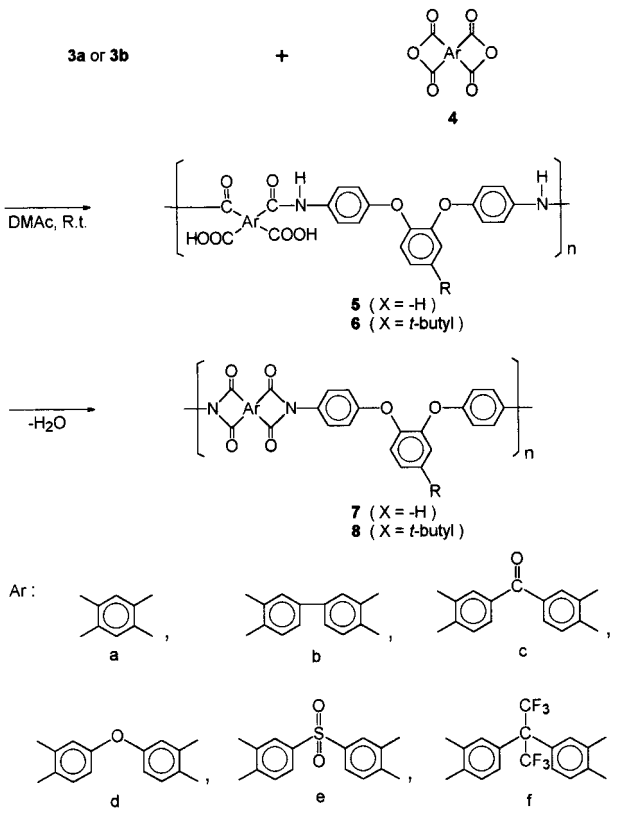

Scheme 2

herent viscosity was carried out without any difficulty, and the inherent viscosities of the soluble polyimides, including **7f**, were in the range of 0.41–0.90 dL/g, as measured in DMAc. The characterization of inherent viscosity for the organic insoluble polyimides was carried out with concentrated sulfuric acid as the solvent. For comparison, the inherent viscosities of the organosoluble polyimides were also characterized in sulfuric acid. As shown in Table I, the polyimides exhibited inherent viscosities of 0.46–1.48 dL/g, as measured in concentrated sulfuric acid. However, in the case of **7b**, there was always some insoluble gel in concentrated sulfuric acid; therefore, no attempts were made to determine its inherent viscosity.

Polymer Characterization

FTIR spectroscopic characterization was performed on thin films. All polyimides exhibited the characteristic imide group absorptions around 1780 and 1720 (typical of imide carbonyl), 1380 (C—N stretch), and 1120 and 725 cm^{-1} (imide ring deformation). The disappearance of amide and carboxyl bands indicates a virtually complete conversion of the poly(amic acid) precursor into polyimide.

Table I. The Inherent Viscosities of the Poly(amic acid)s and Polyimides and the Film Quality of the Polyimides

Poly(amic acid)		Polyimide			
			η_{inh} (dL/g)[b]		
Code	η_{inh} (dL/g)[a]	Code	DMAc	Conc. H_2SO_4	Film Quality
5a	1.63	**7a**	—[c]	1.28	Slightly Brittle
5b	1.86	**7b**	—	s[d]	Flexible
5c	1.10	**7c**	—	0.67	Flexible
5d	0.82	**7d**	—	1.00	Flexible
5e	0.98	**7e**	—	1.48	Flexible
5f	0.93	**7f**	0.90	1.33	Flexible
6a	1.44	**8a**	—	0.87	Slightly Brittle
6b	0.89	**8b**	0.81	0.65	Flexible
6c	1.10	**8c**	—	0.78	Flexible
6d	0.97	**8d**	0.58	0.83	Flexible
6e	0.91	**8e**	0.81	0.84	Flexible
6f	0.78	**8f**	0.41	0.46	Flexible

[a] Measured at a concentration of 0.5 g/dL in DMAc at 30 °C.
[b] Measured at a concentration of 0.5 g/dL at 30 °C.
[c] Insoluble.
[d] Swelling.

Table II. Solubility Behavior of the Polyimides

Polymer Code	Solvent					
	DMAc	NMP	DMF	DMSO	*m*-Cresol	THF
7a	−	−	−	−	−	−
7b	−	+	−	−	+h	−
7c	−	s	−	−	s	−
7d	−	−	−	−	−	−
7e	−	−	−	−	−	−
7f	+	+	+	+	+	+
8a	−	−	−	−	−	−
8b	+	+	+	+	+	+
8c	s	s	s	−	−	s
8d	+	+	+	+	+h	+
8e	+	+	+	+	+h	+
8f	+	+	+	+	+	+

Qualitative solubility was determined with 10 mg of polymer in 1 mL of solvent. + = soluble at room temperature; +h = soluble on heating at 100 °C; s = swelling; − = insoluble even on heating.

All the polyimides revealed an amorphous nature, as evidenced by the X-ray diffraction patterns. The solubility behaviors of the synthesized polyimides were tested qualitatively in DMAc, *N*-methyl-2-pyrrolidone (NMP), DMF, dimethyl sulfoxide (DMSO), *m*-cresol, and tetrahydrofuran (THF), and the results are summarized in Table II. For the **7a–f** series, only the polyimide (**7f**) derived from 6FDA was readily soluble in all the solvents tested. The excellent solubility of polyimide **7f** may be due to its noncoplanar structure and low cohesive energy caused by the CF_3 group. Poor solubility for the other **3a**-based polyimides indicates either strong intermolecular interactions or good packing ability. Solubility was enhanced dramatically with the attachment of a *tert*-butyl group. In addition to the polyimide (**8f**) derived from 6FDA, the polyimides (**8b**, **8d**, and **8e**) obtained from BPDA, OPDA, and DSDA were also readily soluble in almost all the solvents tested. The large differences in solubility between the **7b–e** and **8b–e** series are believed to be related to the molecular asymmetry and the presence of bulky *tert*-butyl groups in **3b**. Molecular asymmetry and the *tert*-butyl group inhibit close packing, thus reducing the interchain interactions to enhance solubility.

The tensile properties of some typical polyimide films are presented in Table III. The values are high, with moduli ranging from 1.88 to 2.38 GPa and tensile strengths between 100 and 118 MPa. Polyimide **7b** behaved as a tough material. It necked during the tensile test and showed a relatively higher extension to break. The introduction of the pendant *t*-butyl group seems to cause a decrease of both strength and toughness because of the volume, which increases the separation between chains and decreases the strength of the intermolecular interactions.

The thermal properties of the polyimides were evaluated by DSC, TMA, and TGA, and the results are listed in Table IV. Polyimides **7b–f** showed T_g values of 222–259 °C by DSC and 212–248 °C by TMA. No T_g value was observed for the polyimide (**7a**) from PMDA by DSC; however, the T_g of polyimide **7a** could be easily detected by TMA. The T_g values for polyimides **8a–f** were recorded in the range of 229–260 °C by DSC and 204–241 °C by TMA. The first heating DSC scan of polyimide **8a** showed a sharp endotherm peak at 354 °C. Rapid cooling and reheating showed a strong T_g at 260 °C and the disappearance of the melting transition, indicative of a low crystalliza-

Table III. Tensile Properties of the Polyimide Films

Polymer Code	Strength-to-Break (MPa)	Elongation at Break Point (%)	Initial Modulus (GPa)
7b	110	54	2.38
7d	118	10	2.37
8b	100	6	1.88
8d	103	6	2.17

Table IV. Thermal Properties of the Polyimides

	T_g (°C)		T_d (°C)[a]		
Polymer Code	DSC	TMA	In Air	In N_2	Char Yield (%)[b]
7a	—	282	581	583	54.9
7b	246	235	573	575	60.7
7c	235	221	573	572	56.4
7d	222	212	546	555	60.2
7e	259	248	556	545	52.6
7f	250	239	558	559	57.3
8a	260(354)[c]	241	530	533	47.9
8b	251	224	551	533	48.2
8c	239	229	535	526	50.6
8d	229	204	528	530	54.4
8e	256	232	513	506	41.2
8f	242	222	541	543	54.5

[a] Decomposition temperature at which a 10% weight loss was recorded by TGA at a heating rate of 20 °C/min.
[b] Residual weight percentage at 800 °C under a nitrogen atmosphere.
[c] The value in the parentheses is the peak temperature of the endotherm in the first DSC heating trace.

tion rate. In all cases, T_g's measured by TMA were slightly different from those determined by DSC. This difference may be attributed to the differing natures of the testing techniques (calorimetric vs thermomechanical responses). Polyimides from OPDA showed the lowest T_g's in both series because of the decreased rotational barriers caused by the flexible ether linkage between two phthalimide units. The introduction of the pendent *t*-butyl group resulted in only small changes in the T_g values obtained from DSC analyses. Thus, the great volume of the substituents may overcome the effect of asymmetry and irregularity introduced with the pendent group, which should lessen T_g. However, in comparison with the T_g values measured by TMA, most of the **7a–f** series polyimides showed a higher value than the corresponding **8a–f** polyimides. This result may indicate that the polyimides containing pendant *tert*-butyl groups exhibit a higher degree of plasticity near T_g than their analogues without *tert*-butyl groups.

Typical TGA thermograms are illustrated in Figure 2. Decomposition temperatures at a 10% weight loss for polyimides **7a–f** ranged from 546 to 581 °C in nitrogen and 545 to 583 °C in air, values comparable to those of commercial polyimides. Slightly lower decomposition temperatures and char yields for the **8a–f** series in comparison with the **7a–f** series might be a result of the existence of less stable aliphatic segments.

CONCLUSIONS

Extended *ortho*-linked bis(ether amine)s (**3a** and **3b**) based on catechol and 4-*tert*-butylcatechol were successfully synthesized in high purity and high yields. The polymerization of these diamines with several different dianhydrides yielded amorphous polyimides that exhibited T_g values of 220–260 °C and showed good thermal stability. The introduction of *t*-butyl groups onto the polyimide backbones led to a significant increase in solubility without an unacceptable detriment to their thermal properties.

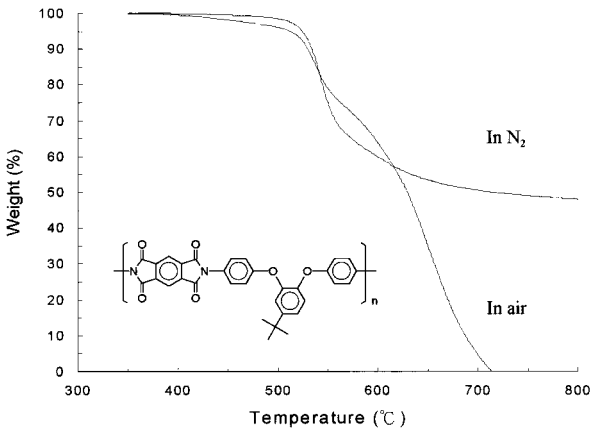

Figure 2. TGA thermograms of polyimide **8a** at a heating rate of 20 °C/min.

The authors thank the National Science Council of the Republic of China for its financial support of this work.

REFERENCES AND NOTES

1. Polyimides; Wilson, D.; Stenzenberger, H. D.; Hergenrother, P. M., Eds.; Chapman & Hall: New York, 1990.
2. Polyimides: Fundamentals and Applications; Ghosh, M. K.; Mittal, K. L., Eds.; Marcel Dekker: New York, 1996.
3. Yamaguchi, A.; Tamai, S.; Ohta, M. Polymer 1996, 37, 3683.
4. Yagci, H.; Ostrowski, C.; Mathias, L. J. J Polym Sci Part A: Polym Chem 1999, 37, 1189.
5. Ayala, D.; Lozano, A. E.; de Abajo, J.; de la Campa, J. G. J Polym Sci Part A: Polym Chem 1999, 37, 805.
6. Hsiao, S.-H.; Dai, L.-R. J Polym Sci Part A: Polym Chem 1999, 37, 665.
7. Liou, G.-S.; Maruyama, M.; Kakimoto, M.; Imai, Y. J Polym Sci Part A: Polym Chem 1993, 31, 2499.
8. Hsiao, S.-H.; Li, C.-T. Macromolecules 1998, 31, 7213.
9. Grubb, T. L.; Ulery, V. L.; Smith, T. J.; Tullos, G. L.; Yagci, H.; Mathias, L. J.; Langsam, M. Polymer 1999, 40, 4279.
10. Li, F.; Fang, S.; Ge, J. J.; Honigfort, P. S.; Chen, J.-C.; Farris, F. W.; Cheng, S. Z. D. Polymer 1999, 40, 4571.
11. Li, F.; Ge, J. J.; Honigfort, P. S.; Fang, S.; Chen, J.-C.; Farris, F. W.; Cheng, S. Z. D. Polymer 1999, 40, 4987.
12. Eastmond, G. C.; Paprotny, J. Macromolecules 1995, 28, 2140.
13. Eastmond, G. C.; Paprotny, J.; Irwin, R. S. Macromolecules 1996, 29, 1382.
14. Akutsu, F.; Inoki, M.; Sawano, M.; Kasashima, Y.; Naruchi, K.; Miura, M. Polymer 1998, 39, 6093.
15. Hsiao, S.-H.; Yang, C.-P.; Chu, K.-Y. Macromolecules 1997, 30, 165.
16. Yang, C.-P.; Chen, W.-T. Macromolecules 1993, 26, 4865.
17. Yang, C.-P.; Chen, W.-T. Makromol Chem 1993, 194, 1595.
18. Yang, C.-P.; Chern, J.-J. J Polym Sci Part A: Polym Chem 1995, 33, 2209.
19. Yang, C.-P.; Oishi, Y.; Kakimoto, M.; Imai, Y. J Polym Sci Part A: Polym Chem 1989, 27, 3895.
20. Yang, C.-P.; Oishi, Y.; Kakimoto, M.; Imai, Y. J Polym Sci Part A: Polym Chem 1990, 28, 1353.
21. Liaw, D.-J.; Liaw, B.-Y. Polym J 1996, 28, 970.
22. Liaw, D.-J.; Liaw, B.-Y. Macromol Symp 1997, 122, 343.
23. Liaw, D.-J.; Liaw, B.-Y. J Polym Sci Part A: Polym Chem 1998, 36, 2301.
24. Yang, C.-P.; Hsiao, S.-H.; Yang, H.-W. Polym J 1998, 30, 723.
25. Yang, C.-P.; Hsiao, S.-H.; Yang, H.-W. Macromol Chem Phys 1999, 200, 1528.
26. Eastmond, G. C.; Paprotny, J. Synthesis June 1998, 894.